UPGRADE PROJECT TO INTRODUCE A PHOTO-INJECTOR INTO t-ACTS AT RARiS, TOHOKU UNIVERSITY*

P. Kitisri[1,†], K. Nanbu[1], F. Hinode[1], S. Kashiwagi[1], T. Muto[2], I. Nagasawa[1], K. Takahashi[1], K. Shibata[1], H. Yamada[1], A. B. Kavar[1], H. Abiko[1], H. Hama[1]
[1]Research Center for Accelerator and Radioisotope Science, Tohoku University, Sendai, Japan
[2]SANKEN (Institute of Scientific and Industrial Research), The University of Osaka, Osaka, Japan

Abstract

The test-accelerator as coherent terahertz (THz) source (t-ACTS) has been routinely producing short electron bunches at the Research Center for Accelerator and Radioisotope Science (RARiS), Tohoku University. According to a theoretical consideration of the pre-bunched Free Electron Laser (FEL) technique, it is expected to produce the THz radiation with extremely high electric fields exceeding 100 MV/cm. In order to achieve the pre-bunched oscillation of FEL, it is required to increase the bunch charge up to 50 pC for the t-ACTS accelerator. However, the maximum bunch charge of the current thermionic RF gun is limited to about 5 pC due to the back-bombardment effect. To overcome this limitation, a project is underway to replace the current thermionic cathode for the RF gun with a photocathode. Currently, the laser system for the photo-injector is being constructed. The system consists of a Yb fiber laser oscillator, a pulse picker, a multi-pass amplifier, and a fourth harmonic generator. The project aims to produce a UV laser with an energy of more than 2 μJ and to achieve a phase difference between the laser system and the RF system of less than 1 degree with respect to a frequency of 2856 MHz. We will present the development status of the laser system, particularly in the sections of the pulse picker and the multi-pass amplifier, to improve the laser pulse shape and laser power.

INTRODUCTION

Research Center for Accelerator and Radioisotope Science (RARiS), Tohoku University, plans to demonstrate a theory of the pre-bunched Free Electron Laser (FEL) in the terahertz (THz) region. The pre-bunched FEL is an FEL technique that utilizes a short electron bunch, with a length of less than the radiation wavelength, as the input beams. That makes the interaction between the synchrotron radiation and electrons more efficient than in a conventional FEL, resulting in nonlinear amplification of the synchrotron radiation intensity [1]. This is expected to be a key of generating a very intense THz light exceeding 100 MV/cm. This intensity is comparable to the electric field between atoms in a crystal lattice, and corresponds to the magnetic field intensity of 33 T that can cause magnetization reversal in metallic ferromagnets, which is the next frontier in nonlinear optics [2].

* Work supported by JSPS KAKENHI Grant Number 23K17306
† pitchayapak.kitisri.p4@dc.tohoku.ac.jp

The test-accelerator as coherent THz source (t-ACTS) has been routinely producing short electron bunches with a length of less than 100 fs, at the RARiS (formerly Research Center for Electron Photon Science) [3], and will be used as a source for the pre-bunched FEL. Even though the electron bunch length meets the requirements for the proof of the theory, the electron bunch charge obtained from the t-ACTS is only 5pC. To prove the theory, including our current experiments, electron beams with a bunch charge of up to 50 pC are required. Since the current RF gun uses a thermionic cathode, raising the cathode temperature leads to an increase in the bunch charge, but also increases the back-bombardment effect. To avoid such an effect at a high bunch charge, a photo-injector project is underway, aiming to replace the thermionic cathode with a photocathode. Moreover, to understand the state inside the FEL cavity in pre-bunched FEL experiments, it is considered to have only one electron bunch in the FEL cavity, and the electron bunch interval needs to correspond to the time that light makes one round trip inside the cavity. Therefore, changing the laser system repetition rate to control the electron bunch interval is much easier than the thermionic RF gun, whose electron bunch interval is determined by the RF frequency of 2856 MHz. To carry out these missions, a laser system is under construction at RARiS [4].

Figure 1 presents the overall systems of this project. The laser system and the synchronization system are under construction. We have finished assembling the Yb fiber laser oscillator and have first tested the synchronization system [4]. In this work, we will present the development status of the laser system.

LASER SYSTEM

A laser system consists of four main sections: Yb fiber laser oscillator, pulse picker, multi-pass amplifier, and the fourth harmonic generator, as depicted in Fig. 1. In this section, we will describe functions and elements of each segment of the laser system.

Yb fiber laser oscillator

A source of a laser is a Yb fiber laser oscillator. The oscillator contains a Yb doped fiber that provides the central wavelength of the laser at around 1035 nm, a half-waveplate (HWP) and quater-waveplates (QWPs) to control mode-lock status, and gratings with piezo to compensate for the dispersion of light with different wavelengths. Figure 2 displays a schematic of the Yb fiber laser oscillator. A polarizing beam

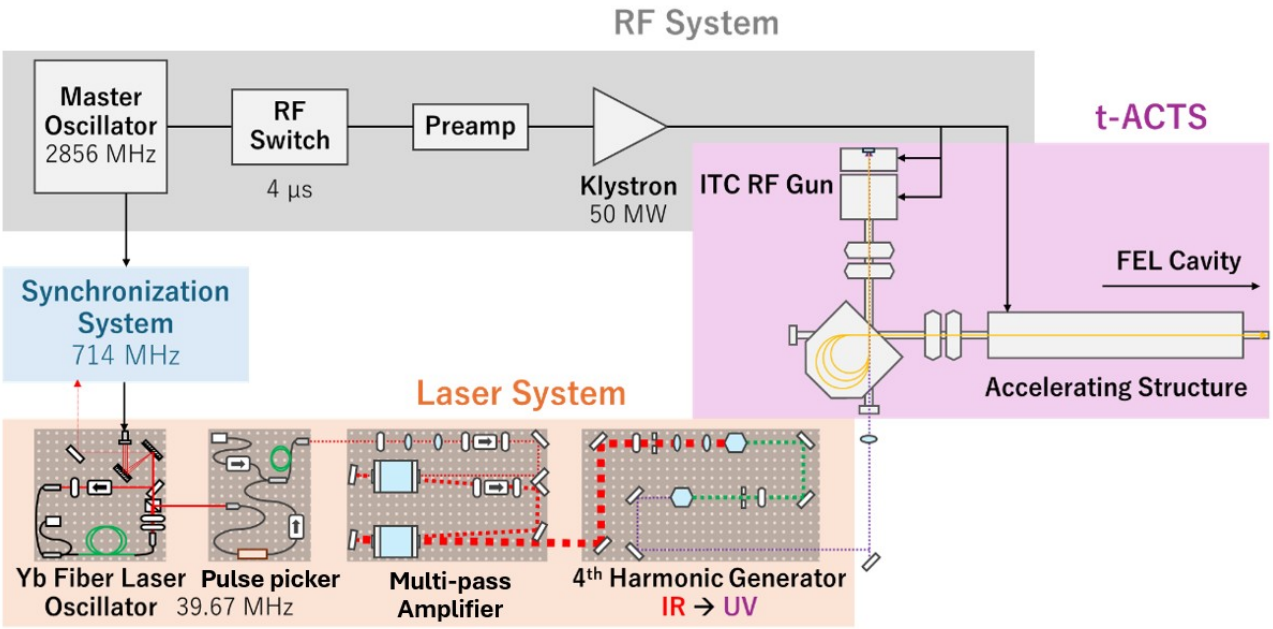

Figure 1: Diagram of the overall systems.

splitter (PBS) in the oscillator splits the laser into two paths, one to the synchronization system and another to the next section of the laser system.

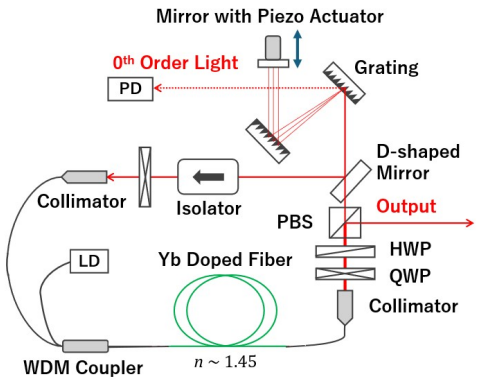

Figure 2: Schematic of a Yb fiber laser oscillator.

Pulse picker

Since the laser generated from the Yb fiber laser oscillator is a continuous wave (CW), to match the RF structure of the accelerator, a pulse picker section is required. This section includes an LN modulator and a pre-amplifier as shown in Fig. 3. The LN modulator convert the laser from a CW waveform to a pulse waveform by splitting the input laser into two paths and recombining them inside it. One path requires an RF signal and a DC-bias signal to change the refractive index of a crystal within it. When the lights from both paths are recombined, the output light from the LN modulator will be constructed or destructed depending on the phase difference between the two paths. Since an applied RF signal is a square pulse with a duration of 2 μs and a repetition rate of 10 Hz, the output light should have the same characteristics.

Before sending the pulsed laser to the next station, the laser will be amplified by the Yb doped fiber. This pre-amplifier needs a pump pulse from a laser diode (LD) that is controlled by a gate signal. The pump pulse will excite electrons of the Yb doped fiber into the excitation state. When the seed laser passes through the fiber during this period, the amplification will occur.

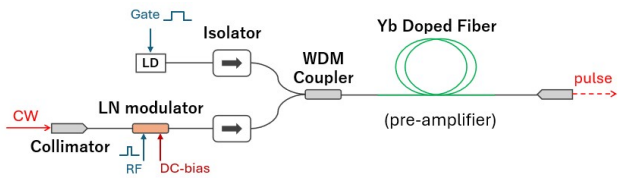

Figure 3: Schematic of a pulse picker section that includes an LN modulator and a pre-amplifier.

Multi-pass amplifier

The pulsed laser from the previous segment comes to this section to be amplified and become a high-power laser. This section consists of two optical amplifiers as depicted in Fig. 4. Each one of them is set up for double-pass amplification, whereby the laser beam traverses each amplifier twice to enhance the gain. An isolator is required upstream of each amplifier to protect the laser source from back-reflected light caused by misalignment. As the optical isolators require a specific linear polarization plane, a QWP is used to convert circularly polarized light into linearly polarized light, and an HWP is used to adjust the polarization plane.

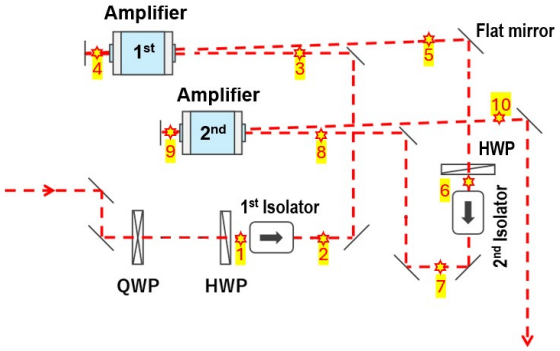

Figure 4: Layout of a Multi-pass amplifier section. Yellow stars with numbers indicate the locations where laser power measurements were performed.

Fourth harmonic generator

The high-power laser from the multi-pass amplifier will travel to this section. Figure 5 illustrates a layout of the fourth harmonic generator. This section has two BBO crystals to perform a second harmonic generation (SHG) twice. The SHG will occur under conditions where an extremely high-power laser interacts with the BBO crystal in the right orientation and proper laser propagation characteristics (generally a focusing laser). The BBO crystals are mounted on a rotation stage. This stage and an HWP help to achieve the proper orientation handily, while lenses serve to modify the laser propagation characteristics.

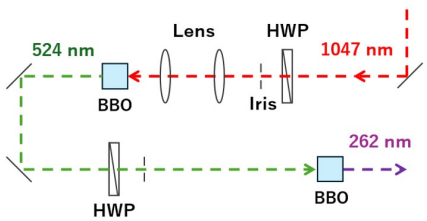

Figure 5: Layout of the fourth harmonic generation.

LASER DEVELOPMENT STATUS

In this topic, we will present the laser measurement and optical element investigation, and update the development status.

Measurement of laser spectrum

After completing the construction of the Yb fiber laser oscillator, we characterized the generated laser spectrum by using a spectrometer at the end of the pre-amplifier. The laser spectrum was measured each time the laser system was operated, over a period of about one month. Table 1 presents the collected data from the laser spectrum measurements.

From the results, the spectral width and central wavelength of the laser are 31 nm and 1037 nm, respectively. It confirms that the laser generated from the Yb laser oscillator has a spectrum covers the amplifier's operating wavelength, which is 1047 nm.

Table 1: Laser spectrum data collected from 12 measurements during approximately one month.

Date	**Laser wavelength (nm)**		
	min	**central**	**max**
09/05/2025	1017	1034	1051
13/05/2025	1017	1035	1052
16/05/2025	1026	1041	1055
23/05/2025 (day)	1028	1042	1055
23/05/2025 (night)	1027	1041	1054
29/05/2025	1022	1037	1051
30/05/2025	1026	1038	1050
06/06/2025	1019	1036	1052
10/06/2025	1017	1035	1052
11/06/2025	1020	1036	1052
12/06/2025	1019	1036	1052
13/06/2025	1019	1036	1052
Average	**1021**	**1037**	**1052**

Measurement of laser polarization

In the pulse picker section, the LN modulator requires a specific polarization plane of the input laser for effective operation. In this experiment, we tested the polarization plane of the laser at the entrance of the LN modulator by using the polarizer and power meter as shown in Fig. 6. A connector in this figure has a keyseat that perfectly fits with a key of the LN modulator's connector. The polarization plane of the input laser should be aligned with this keyseat. We tested the polarization plane by setting the keyseat at the zero degree of the polarizer. Then, we rotated the polarizer and measured the laser power after it passed through the polarizer.

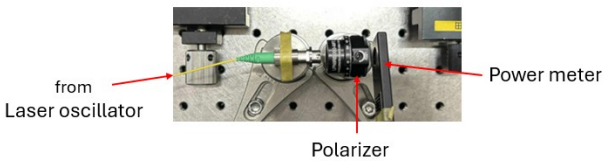

Figure 6: Setup of polarization measurement.

Figure 7 reveals the changed power of the laser when it goes through the polarizer with different angles. As shown in the result, the average power reaches the maximum value at the polarizer's angle of 0° and 180°. It confirms that the laser polarization plane aligns with a key, which corresponds to the LN modulator's requirement.

Timing optimization for a pre-amplifier

It is necessary to optimize the time duration and time delay between the pump pulse and laser pulse for a pre-amplifier to achieve a square laser pulse with a high gain of amplification. In this experiment, we varied the duration of a gate signal for a laser diode (LD) in Fig. 3 and varied the time delay between this signal and the RF signal of the LN modulator. Then, the longitudinal distributions of the pump pulse and

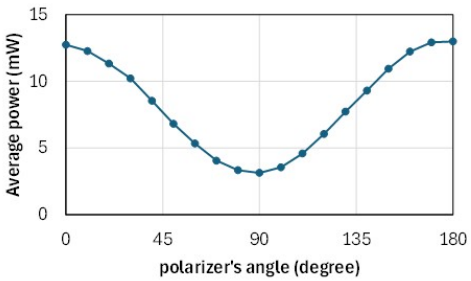

Figure 7: Average power of laser from oscillator after passing through a polarizer with different angles.

the laser pulse were observed by using a photodiode and an oscilloscope at the end of the pulse picker section.

Results are presented in Fig. 8. The duration of the gate clearly affects the length of the pump pulse, but the increasing time of the pump pulse remains the same at about 100 µs before saturating. We can get a high gain of amplification when the laser pulse passes through the fiber at a time that match with the end of the increasing time of the pump pulse or at the beginning of the saturation. Noted that, for achieving a square shape of the laser pulse, the pump pulse should be as short as possible while still giving a high amplification gain. Thus, in this experiment, the proper case is the case that uses the gate duration of 300 µs and delay time between the gate signal and the RF signal of 300 µs.

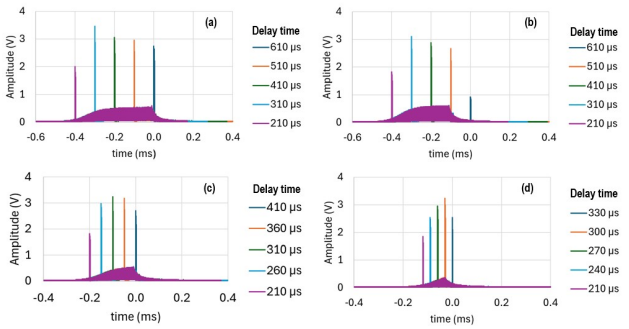

Figure 8: Longitudinal distributions of pump pulse (base) and laser pulse (spikes) from pre-ampilfier with different delay times at gate duration of (a) 600 µs, (b) 500 µs, (c) 400 µs, and (d) 300 µs.

Optimization of an LN modulator

Once the proper duration of the gate signal and the delay time between the gate pulse and the RF pulse of the LN modulator are achieved, applied voltages for the RF port and the DC-bias port of the LN modulator are investigated. The RF signal controls the shape and amplitude of the output laser pulse, while the DC bias voltage affects the amplitude ratio between the pulse region (RF on-time) and the interval between pulses (RF off-time).

In this experiment, we varied the RF voltages along with the DC-bias voltage and measured the laser longitudinal distribution at the end of the pre-amplifier with the photodiode and the oscilloscope. Figure 9(a) displays the longitudinal distribution of the laser when the DC-bias voltage of 0.002 V was applied with different RF voltages. The results indicate that applying the RF voltage of 3.00 V provides the laser pulse with the maximum amplitude.

Then, the RF voltage of the LN modulator was fixed at the value of 3.00 V and the DC-bias voltage was applied with different positive values and negative values as shown in Fig. 9(b) and 9(c), respectively. They expose that applying the DC-bias voltage close to zero yield the maximum amplitude of the laser pulse.

Finally, the laser distribution applied the RF voltage of 3.00 V and the DC-bias voltage of 0.002 V was compared with the DC-bias voltage of −0.002 V as seen in Fig 9(d). It reveals that applying a small negative value of the DC-bias voltage provides a laser pulse amplitude higher than applying the DC-bias voltage with positive values. Moreover, it gives the minimum amplitude at the time between the laser pulses (during off time of the RF signal).

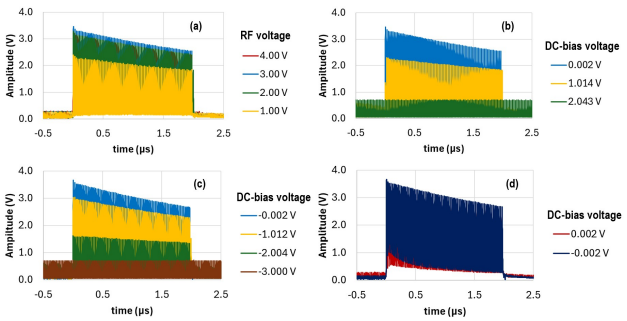

Figure 9: Longitudinal distributions of the laser pulse with different configurations of the LN modulator: (a) DC-bias voltage of 0.002 V with different RF voltages, (b) RF voltage of 3.00 V with different positive value of DC-bias voltage, and (c) RF voltage of 3.00 V with different negative value of DC-bias voltage. (d) A comparison of the laser distributions when applied RF voltage of 3.00 V with DC-bias voltage of 0.002 V and −0.002 V.

Alignment of the low-power laser

We aligned the laser orbit in the multi-pass amplifier section without operating amplifiers, so it is called low-power laser alignment. All of the optical elements in Fig. 4 are mounted on an optical table. Every elements were aligned to make sure that the laser could travel through them with high transmission efficiency before interacting with the BBO crystal in the next section. The laser pulse came from the pulse picker section to this section with the infrared (IR) wavelength. A laser detection card for IR wavelength (IR card) was used to observe the laser beam during the alignment, along with the power meter. Table 2 shows the average powers of the low-power laser measured at various positions along the multi-pass amplifier section after completing the alignment.

In this experiment, the RF repetition rate of the LN modulator was set at 20 Hz to make the laser beam clearly visible on the IR card, except at positions 8, 9, and 10, where it was set at the general rate of 10 Hz.

Table 2: Average powers of the low-power laser measured at different positions along the multi-pass amplifier section after alignment completion.

Position	Average power (mW)	Transmission
1	2.10	
2	1.87	89%
3	1.87	
4	1.87	100%
5	1.72	92%
6	1.66	
7	1.37	83%
8*	0.92	
9*	0.92	100%
10*	0.87	95%

According to the alignment results, we could achieve the alignment for the first and the second isolators with 89% and 83% transmissions, respectively. For the first amplifier, we reached the transmission percentages of 100% and 92% for the first pass and the second pass, respectively. Lastly, the transmission efficiencies of the second amplifier were 100% and 95% for the first pass and the second pass, respectively.

Test of the high-power laser

When the low-power laser alignment was completed, we operated the amplifiers in the multi-pass amplifier section to test the high-power laser. However, we encountered a problem with the first amplifier. The pump pulse of the first amplifier leaked and traveled along with our seed laser. The mixing between the pump pulse and the laser pulse caused to a large laser size over 12.7 mm (0.5 inch) from about 2 mm. Subsequently degenerated the laser characteristics and invalidated the low-power laser alignment.

Next step, an iris will be placed downstream of the first amplifier (Fig. 4 position 4) to filter out the pump pulse, allowing only the laser pulse to proceed. We expect to achieve good results and then move on to the fourth harmonic generator section.

CONCLUSION AND FUTURE PLANS

The photo-injector project is undergoing for the t-ACTS at the RARiS, and the laser system is under construction. The laser system consists of a Yb fiber laser oscillator, a pulse picker, a multi-pass amplifier, and a fourth harmonic generator. The Yb fiber laser oscillator was successfully constructed and confirmed to generate an IR laser with a spectral width and central wavelength of 31 nm and 1037 nm, respectively. This wavelength covers the operating wavelength of the multi-pass amplifier. As well, the polarization plane of the IR laser was confirmed to meet the requirements of the LN modulator in the pulse picker section.

A pre-amplifier in the pulse picker section was investigated for the timing optimization. The optimized duration of a gate signal for the pump pulse is 300 µs, and the RF signal of the LN modulator should be delayed from the gate signal for 300 µs. With these configurations, the laser pulse will match at the end of the rising time of the pump pulse. This leads to the maximum amplification gain while keeping the pump pulse short to minimize amplitude at the time between the laser pulses.

Then, the applied voltages for the RF port and DC-bias port of the LN modulator were optimized. The configurations of the RF voltage and the DC-bias voltage should be investigated to achieve the square shape of the laser pulse. In this setup, the optimized values of the RF voltage and the DC-bias voltage are 3.00 V and −0.002 V, respectively.

Finally, every optical element in the multi-pass amplifier section was aligned with the low-power IR pulsed laser. The alignment of the low-power laser was completed with at least 80% transmission for all elements. However, it was invalidated when we operated the high-power laser due to a leakage of a pump pulse of the first amplifier.

As the next step, an iris will be placed downstream of the first amplifier to filter out the pump pulse, allowing only the amplified IR pulsed laser to pass through and proceed to the fourth harmonic generator. Furthermore, the section of the fourth harmonic generator will be aligned and investigated to achieve the generation of a UV laser with an energy of more than 2 µJ.

ACKNOWLEDGEMENTS

We would like to thank Associate Professor Kazuyuki Sakaue of the University of Tokyo for his extensive support in constructing the laser system.

We would like to thank Mr. Kodai Kudo for his contributions during the early stages of this project, particularly in the Yb fiber laser oscillator section.

REFERENCES

[1] H. Hama *et al.*, "Intense coherent terahertz generation from accelerator-based sources," *NIM-A*, vol. 637, no. 1, pp. S57–S61, 2011.

[2] A. D. Koulouklidis *et al.*, "Observation of extremely efficient terahertz generation from mid-infrared two-color laser filaments," *Nat. Commun.*, vol. 11, no. 1, p. 292, 2020.

[3] S. Kashiwagi *et al.*, "Status of Test-Accelerator as Coherent THz Source (t-ACTS) at ELPH, Tohoku University," in *Proc. IPAC'19*, ser. IPAC, no. 10. JACoW Publishing, Jun. 2019, paper TUPGW033, pp. 1475–1477, https://doi.org/10.18429/JACoW-IPAC2019-TUPGW033.

[4] H. Hama *et al.*, "Development of photo injector employing yb fiber laser for stimulus super-radiant thz fel," in *Proc. IPAC'25*, ser. IPAC, no. 16. JACoW Publishing, Jun. 2025, paper TUPM029, pp. 1224–1226. [Online]. Available: https://indico.jacow.org/event/81/contributions/7661